Radiation Physics and Chemistry 122 (2016) 24–27

Contents lists available at ScienceDirect

Radiation Physics and Chemistry

journal homepage: www.elsevier.com/locate/radphyschem

Angular distributions of differential X-ray production cross sections for Cu and Ta in photoionization

Xing Wang *, Zhongfeng Xu, Lin Cheng

School of Science, Xi'an Jiaotong University, Xi'an 710049, China

HIGHLIGHTS

- The typical X-rays have been measured with a secondary-target system.
- The experimental setup provides us more choice to select incident energy.
- The discrepancy of the X-ray production ratios is determined experimentally.

ARTICLE INFO

Article history:
Received 9 October 2015
Received in revised form
20 December 2015
Accepted 12 January 2016
Available online 13 January 2016

Keywords:
X-ray
Angular distribution
Cross section
Vacancy

ABSTRACT

The characteristic K-shell X-ray emission of Cu and L X-rays of Ta in photoionization has been measured at excitation energy of 15.9 keV. The differential X-ray production cross sections of K_α and K_β for Cu and L_α, $L_{\beta1}$, $L_{\beta2}$, $L_{\gamma1}$ for Ta are derived at emission angles ranging from 100° to 150°. The ratio of K_β and K_α X-ray production cross sections, K_β/K_α, is calculated for Cu and it is found to be consistent with other work even at different incident energy. While the ratios of L_α/L_β, $L_\alpha/L_{\gamma1}$ and $L_\beta/L_{\gamma1}$ for Ta are found to be different with other results at different excitation energy. The reasons giving rise to this discrepancy are clarified with thorough analysis.

1. Introduction

Inner-shell ionization of atoms has been extensively investigated through the radiation channel leading to characteristic X-rays emission from atomic shells for several decades (Schuch et al., 2000; Limandri et al., 2008; Wang et al., 2015; Bambynek et al., 1972; Wang et al., 2013). It is a well-known physical analytical method to identify elements by their characteristic X-rays in chemical, environmental and geological fields (Šmit, 2005). The emission of X-rays in photoionization is a fundamental process of interaction of photons with matters (Yalçın et al., 2008; Wang et al., 2014).

The precise measurement of ionization cross sections plays an important role in many practical fields, so it is supposed to be considered that whether the emission of X-ray or Auger electron is isotropic in collision process. There are two predictions on the alignment for vacancy state in impact collision process. One view predicts that vacancies created by impact ionization in states with $j > 1/2$ are aligned and X-rays (or Auger electron) emission following the decay of vacancies are anisotropic and polarized (Flügge et al., 1972); While the other view, which contradicts the above one, predicts that vacancy states produced by impact ionization with $j \geq 1/2$ are unaligned and accordingly the emission of X-rays (or Auger electron) is isotropic and unpolarized (Cooper and Zare, 1969). A lot of experiment has been implemented to study the alignment behavior of vacancy states, by measuring the polarization or angular distribution of typical X-ray lines (Salem et al., 2013; Raza et al., 2013; Özdemir et al., 2011; Han et al., 2009; Kumar et al., 2010; Tartari et al., 2003; Gonzales et al., 2012). It is demonstrated that the decay of vacancy state with $j > 1/2$ presents an anisotropic X-ray emission from some experimental results (Salem et al., 2013; Raza et al., 2013; Özdemir et al., 2011; Han et al., 2009); while other groups have observed the isotropic angular distribution of X-ray emission via the decay of vacancy state with $j > 1/2$ (Kumar et al., 2010; Tartari et al., 2003; Gonzales et al., 2012). Therefore, further theoretical and experimental studies are called for to investigate the alignment behavior of vacancy states with $j > 1/2$.

Most measurements are performed to study the angular distribution of X-ray emission with radioisotopes. While in this work, the experiment has been implemented with an X-ray tube with a secondary-target system as the excitation source instead of

* Corresponding author.
E-mail address: wangxingcn@mail.xjtu.edu.cn (X. Wang).

http://dx.doi.org/10.1016/j.radphyschem.2016.01.016

radioactive sources. In the secondary-target system, the primary bremsstrahlung radiation produced by the electrons is utilized to excite the secondary target (Zr, in this work). Therefore, it is possible to eliminate the continuous spectra of bremsstrahlung radiation produced by the first target (Ag, in this work) and generate monochromatic X-rays with high intensity. Besides the easier control of the intensity of incident photons, it also provides us the choice to select more incident energies of photons (Rao et al., 1993). Here, we report the experimental study on angular distribution of K X-rays for Cu and L X-rays for Ta produced by 15.9 keV X-rays at backward angles ranging from 100° to 150°. The typical X-ray intensity ratios are derived and compared with other experimental data.

2. Methods and measurements

The experiment has been implemented to study the angular dependence and branching ratios of X-ray emission bombarded by X-rays with energy of 15.9 keV. The geometry of experimental setup is depicted in Fig. 1. An X-ray tube (Mini-X, AMPTEK Inc., USA) worked with 0.75 μm silver target is employed as the primary radiation source. The bremsstrahlung spectrum produced by X-ray tube at acceleration voltage of 30 kV and current of 90 μA is collimated by a Zr tube with inside diameter of 2 mm. Then the collimated bremsstrahlung X-rays impact on a secondary target of element Zr. The typical K X-ray spectrum of Zr can be considered as a single and symmetric peak centered at 15.9 keV. The K X-rays of Zr should be unpolarized (filling of vacancy in K_1 shell, $j=1/2$). This energy can also be obtained by calculating the weighted average of K_α and K_β X-ray energies according to their intensity ratio. Fluorescent X-rays generated from the secondary target are collimated to irradiate on the Cu and Ta sample perpendicularly. The thicknesses of Cu and Ta samples are 22.4 mg cm^{-2} and 166.5 mg cm^{-2}, respectively. Finally, an AMPTEK production Silicon Drift Detector (XR-100SDD) is employed to measure the typical X-rays emitted from the sample at emission angles from 100° to 150°. Here, the X-ray detector is removable while other parts are fixed. The detection solid angle is 1.1×10^{-3} sr. The detector has an active crystal size of 25 mm^2 and a resolution about 125 eV at 5.9 keV. The detector is placed at the position of sample in advance to determine the counts of incident X-rays per second and per unit area. In order to accumulate sufficient photon count, all the spectra were measured more than 1200 s intervals.

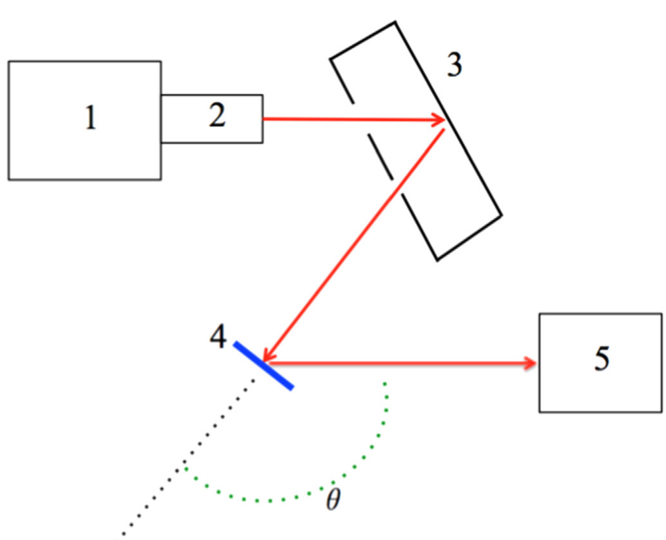

Fig. 1. Schematic diagram of experimental setup. (1) X-ray tube; (2) Zr collimator with inside diameter of 2 mm; (3) Secondary target of element Zr; (4) Sample; (5) Removable X-ray detector. The emission angle is denoted by θ.

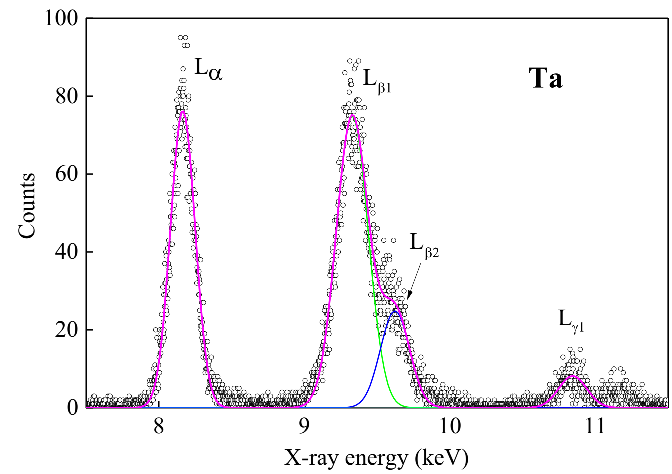

Fig. 2. Characteristic L X-ray spectra of Ta induced by 15.9 keV X-rays at emission angle of 140°.

3. Results and discussions

Fig. 2 shows the measured typical L X-ray spectra of Ta at emission angle of 140°. It is found that the peak energies of $L_{\alpha1}$ (L_3M_5) and $L_{\alpha2}$ (L_3M_4) X-rays are too close to be resolved. While the L_α ($L_3M_{4,5}$), $L_{\beta1}$ (L_2M_4), $L_{\beta2}$ (L_3N_5) and $L_{\gamma1}$ (L_2N_4) X-rays of Ta can be separated clearly with multi-peak Gaussian fitting procedure.

The differential cross section for the X-ray emission at emission angle θ is given by Demir et al. (2003)

$$\frac{d^\theta\sigma}{d\Omega} = \frac{N_x^\theta}{S_x a_x (N/M)\varepsilon\omega^\theta t\beta^\theta} \tag{1}$$

where S_x is the number of incident X-rays received by the surface of the target per second; N_x^θ is the number of X-rays detected per second under the X-ray peak at an emission angle θ with the incident beam; a_x is the correction coefficient due to absorption of characteristic X-rays of sample in the air column between target and detector; ε is the efficiency of the detector; M is atomic weight and N is Avogadro's constant; t is the thickness of the target in g/cm^2; ω^θ is the target-detector solid angle; β^θ is the target self-absorption correction factor of incident and emitted X-rays, and it can be calculated with the formula

$$\beta^\theta = \frac{1-\exp\left[-(\mu_{inc}\sec\theta_1 + \mu_{emt}\sec\theta_2)t\right]}{(\mu_{inc}\sec\theta_1 + \mu_{emt}\sec\theta_2)t}, \tag{2}$$

Here μ_{inc} (cm^2 g^{-1}) and μ_{emt} (cm^2 g^{-1}) are the mass absorption coefficients for incident and emitted radiation, respectively (http://www.nist.gov/pml/data/xraycoef/); θ_1 and θ_2 are the angles of incident photons and emitted X-rays with respect to the normal at the surface of the target, t is the mass thickness of target (g cm^{-2}). The calculated values of self-absorption correction factor β^θ are presented in Table 1. Due to relatively thinner target thickness, the self-absorption correction factor for Cu is much larger than that for Ta.

Combining statistical error (3%) with errors estimated for solid angle (6%), background subtraction (3%) and fitting procedure (4%), the total experimental error for X-ray production cross section in this work is less than 11%. Fig. 3 presents the angular distribution of differential cross sections of the K_α and K_β X-rays for Cu. It can be seen that the emission of K_α and K_β X-rays are essentially